

Convective Blockage during Earth Re-entry. A review.

Philippe Reynier¹

Ingénierie et Systèmes Avancés, Mérignac, 33702, France

During entry, the decomposition of the TPS material resin by the pyrolysis process produces blowing gases that are injected in the boundary layer. Induced by the blowing gas, the blockage phenomenon has a strong effect on the level of heat-fluxes during entry. For example, during the preparation of the Stardust mission, numerical simulations have established a decrease of 35% of the heat-flux at the stagnation point when the blockage was accounted for. This phenomenon is strongly link to turbulence and to the porous aspects of the material. As a consequence, for some planetary entries and Earth super-orbital re-entries characteristic of sample return missions, blockage is one of the key issues that have to be addressed. Here, the experimental, numerical and flight data obtained for different missions involving high level of heat-fluxes are gathered and discussed. The models for convective blockage found in the literature have been reviewed in order to propose a generic way to estimate this phenomenon.

I. Introduction

In the frame of its science and exploration programmes, the European Agency is studying several missions such as the Jupiter Entry Probe (JEP), the European Vehicle Demonstrator (EVD) and a sample return mission to Mars involving a high speed Earth re-entry of the sample return capsule. These missions are characterized by severe entries into Jupiter and Earth atmospheres with high heat-loads and heat-fluxes. In each case, the radiative heat-flux is high and for the Jovian entry most of the heat-flux is radiative.

For such entries, the thermal protection system is made of ablative material able to sustain the high heat-load. The ablative material is pyrolysed and the gases produced by the material decomposition are blown in the boundary layer surrounding the capsule as resumed by Lau and Venkatapathy¹ in Fig. 1. The blowing phenomenon has for effect to block a part of the heat-flux coming from the high temperature shock layer. This phenomenon called blockage can reduce drastically the convective and/or radiative heat-flux: For Galileo most of the convective heat-flux was blocked by the strong blowing. The convective blockage depends mainly on the blowing rate of the pyrolysis gas and as a consequence on re-entry conditions and material properties. The radiative blockage is function as the species blown in the boundary layer, species like C_2 and C_3 are known for their absorption capabilities.

There is little material in the literature focusing exclusively on blockage: the available data is sparse without any extensive study focusing on this phenomenon. However, some published flight data are available for Apollo 4, Pioneer-Venus and Galileo which have been reviewed and analyzed by Park and Tauber². The Galileo mission prepared by NASA in the seventies has driven some activity on the blockage phenomenon. In the last years, the development of several sample return capsules by NASA and JAXA such as Genesis, Muses and Stardust has induced a revival of the investigations on blockage.

The objective of this review is to gather the literature data available on blockage with a focus on the convective blockage for a high-speed Earth entry. However, since the first elements found in the literature on this topic, date back from the Galileo project, the heritage of this mission is a part of the review. The following part focuses on the Pioneer-Venus mission and has been included due to the similarity between the Venus entry and a super-orbital Earth entry. The results found on the high speed Earth re-entries performed have been reviewed with the heritage of Apollo 4 and the experience gained recently on Genesis, Muses and Stardust. The last part is dedicated to the modelling of the convective blockage factor. An important point to be assessed is the blowing rate of the material. A critical review of the existing models to estimate this quantity from material properties and entry characteristics is performed.

¹ Research Engineer, ISA, BP 20005, 19 Allée James Watt, 33703 Mérignac, France, Philippe.Reynier@isa-space.eu

II. Galileo Heritage

Many studies have been focused on the TPS and the aerothermodynamics of Galileo from the mid-seventies to recently. First papers, on the mission preparation, date back from the seventies to the early eighties, while the last ones focus on the post-flight analysis, since the Galileo heat-shield was equipped with ablation detector sensors and thermometers.

Due to very high radiative and convective heat-fluxes characterizing a Jupiter entry, the dominant uncertainty factor associated to the heat shield recession calculations was the radiation absorption within the ablation layer. As a consequence, for this mission, the evaluation of the blockage (convective and radiative) was a major issue. Among the different studies, some papers have provided some estimate on the blockage factors and blowing rates estimated for a Jupiter entry.

A. Convective blockage

The convective blockage depends mainly on the mass injection rate which is directly proportional to the surface heating rate. Usually, the ablation process is assumed to be steady and the wall temperature is the sublimation temperature of the ablator surface. For Galileo entry, due to a massive blowing³, the stagnation point convective heat-flux was reduced to zero during most of the radiative heating pulse⁴. This reduction of the convective heat transfer to an insignificant level is illustrated in Fig. 2. In this figure, the peak of the convective heat-flux at the stagnation point is shifted in time: with the end of the entry pulse, the blowing becomes weaker and the convective heating is not completely offset (the blowing efficiency depends also on the ratio between the mass-flow-rates of the pyrolysis gas and the freestream mass flux). On the frustum (right part of Fig. 2), the carbon phenolic was submitted to a severe thermal environment with a turbulent convective heating representing 1/3 of the total incident heat-load⁵. As at the stagnation point, the peak of convective heat-flux is shifted in time under the blowing effect.

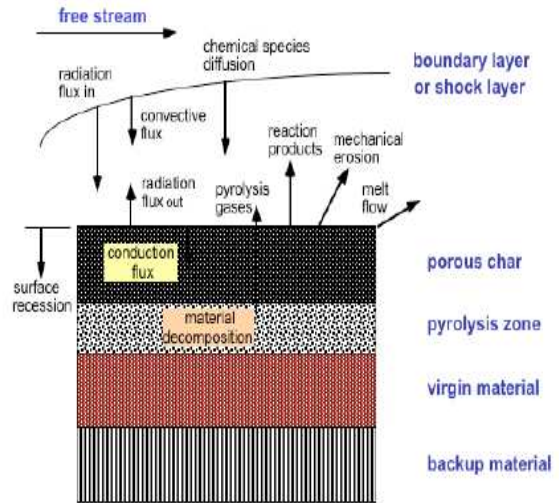


Figure 1: Energy accommodation mechanisms of ablative materials (from Ref. 1)

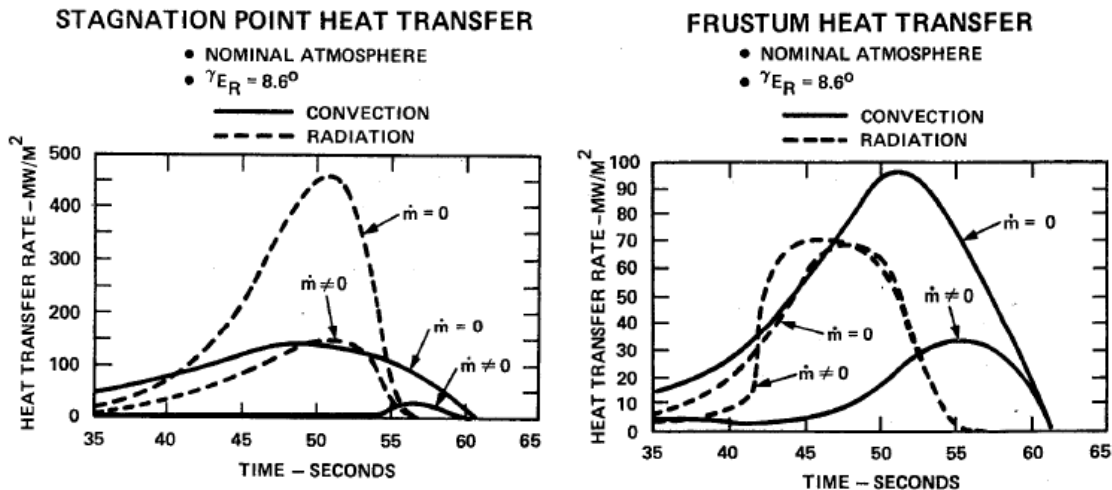


Figure 2: Stagnation point and frustum heat transfer with and without mass flow injection (from Ref. 5)

A first correlation for the convective blockage has been proposed by Brewer et al.⁶ based solely on laminar boundary layer flow solutions. Another correlation has been developed for turbulent flows⁵. In this correlation, shown in Fig.3, the turbulent convective blockage factor, ψ_{CT} , is represented as function of the blowing coefficient

($B' = \dot{m}/C_w$, where \dot{m} is the injection rate and C_w the convective heat transfer). Using this correlation the convective blockage is given by,

$$\psi_{C_T} = \left[\frac{2.344}{B'} (\sqrt{B'+1} - 1) \right]^{1.083} \quad (1)$$

Compared to laminar flow solutions, the turbulent flow solutions⁵ show less blocking effectiveness for both convective and radiative heat transfer. Numerical simulations⁷⁻⁸ showed that the turbulence has a pronounced adverse effect on the surface heating.

The numerical simulations with ablation injection^{7,9} demonstrated that the blowing rates were of such magnitude (see Fig. 4), that the turbulent convective heating values were small comparing to the radiative values but yet significant since they were approximately 10% of the radiative values on the conical frustum

B. Radiative Blockage

The first evaluations¹⁰⁻¹¹ of the radiative blockage showed that for Jupiter entry studies, the ablation species injected in the shock-layer block over 50% of the radiation. For one of the cases computed by Moss et al.⁴, the continuum flux incident at the ablation layer edge was reduced from 380 MW/m² to 149 MW/m². The line radiation was reduced from 229 MW/m² to 64 MW/m² at the wall. For the less severe case the radiative flux was decreased by 63%.

The radiative blockage has been shown⁴ to be large and primarily dependent upon the absorption of C₂ and C₃ species. The calculations performed by Moss et al.⁴, were performed to build a stagnation-point correlation for the blockage factor valid for a large range of entry conditions that can be used for parametric studies. This correlation shows that for Jovian entry conditions, as much as 80% of the radiation blocked is due to the absorption of C₂ and C₃ molecules. Fig. 5 represents a comparison of the stagnation point radiative blockage factors obtained for the calculations of Moss et al.^{4,11}. The results show the same trend so that the radiative blockage factor increases as the magnitude of the radiative heating without injection increases.

Most of the radiative flux reduction is the result of absorption by C₂ and C₃ species. At the beginning of Galileo project, absorption properties of many of the ablation products (C₂H, C₃H and C₄H) were in-existent or very limited as for C₃. The use of new data for the ablation products⁹, such as C₂H, C₃H and C₄H produces a substantially higher

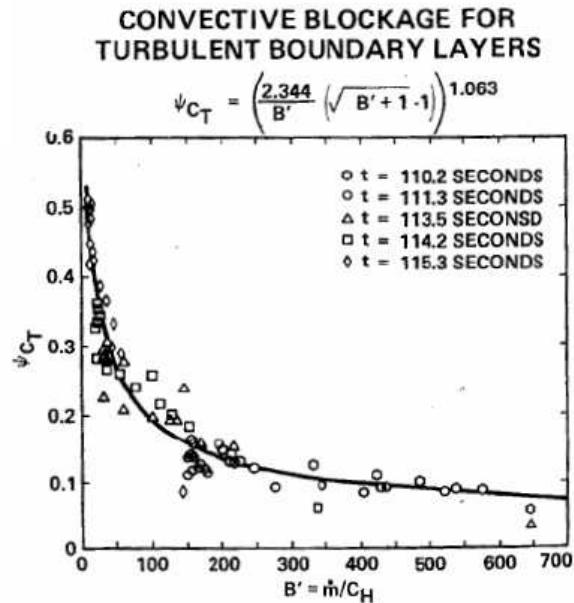


Figure 3: Convective blockage for turbulent boundary layers (from Ref. 5)

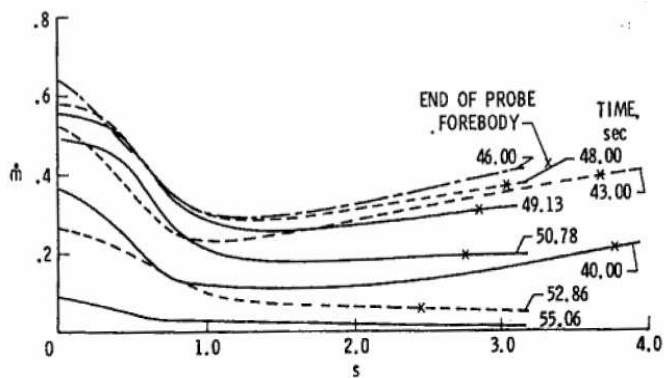


Figure 4: Non dimensional mass injection rate (from ref. 9)

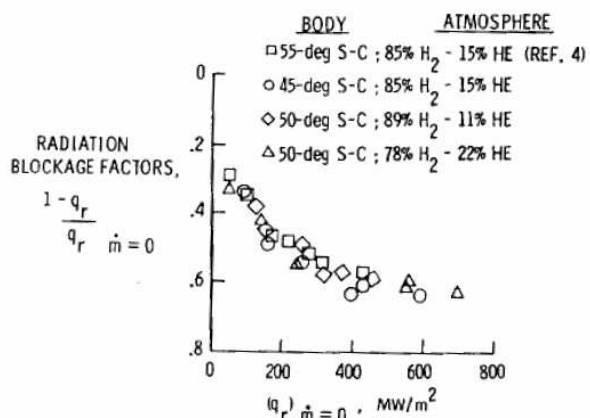


Figure 5: Radiative blockage for coupled carbon-phenolic injection (from Ref. 4)

sublimation enthalpy than previously. The radiation absorption was massively dependent on C_2 and C_3 species which exist in the relative cool portion of the ablation layer. The density numbers calculated for these species were function of the temperature-dependent thermodynamic properties. Jones¹² had concluded that the uncertainty on C_3 properties, combined with significant variations in the measured heat of formation, produced rather large variations in the computed concentration of C_3 .

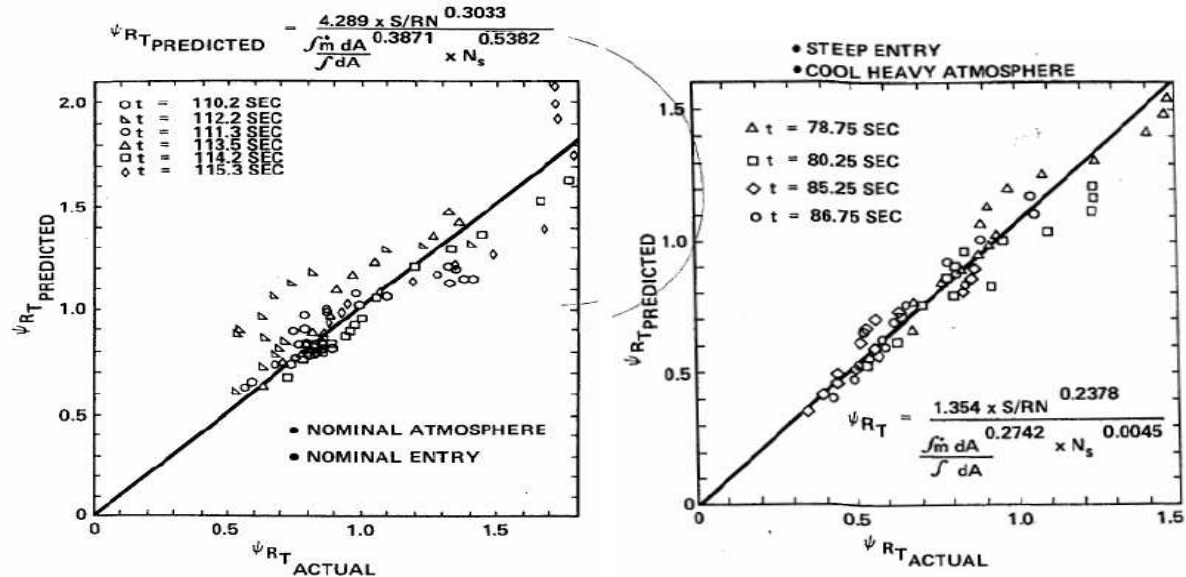


Figure 6: Radiation blockage correlations and data for nominal entry and atmosphere (left); on the right, step entry and cool heavy atmosphere (from Ref. 5)

The C_3 absorption was significant, particularly when new experimental data¹²⁻¹³ for C_3 spectral absorption properties was used^{4,7}. Since there was some uncertainty on the data used for C_3 , several investigations¹²⁻¹⁴ were performed to provide supplement values, particularly for the C_3 Swings bands. The set of data has a large influence⁴, as in the calculations made with Brewer and Engelke's¹⁵ C_3 data; the calculated radiative flux is 17% higher than with the Jones's data¹²⁻¹³. According to Moss et al⁴, the carbon-phenolic injection blocks essentially all the radiation from the Lyman lines, a significant portion of the radiation from the Balmer lines and has a negligible effect on the radiation from the lower hydrogen line series. The same study shows that one band for C_3 absorbs more of the radiation penetrating the ablation layer than the C_2 bands (Swan, Mulliken, Freymark, and Fox-Herzberg).

The laminar solutions¹¹ showed that the blockage factor on the flank of a 50° hyperboloid was slightly higher than the corresponding stagnation point values. This would induce a blockage factor near 60%. The large blockage factors may be reduced if turbulence occurs and would be reduced if radiative non equilibrium due to saturation occurs.

Correlations for the radiative blockage factor, ψ_{RT} , have been proposed for two Jupiter model atmospheres⁵ using turbulent flow calculations and are shown in Fig. 6. This kind of correlation is only valid at the stagnation point and cannot be applied downstream of the stagnation region¹¹. These correlations are expressed as a function of local body position (S/R_N), shock stand-off distance (N_s) and an average mass addition rate (where A is the section area and the \dot{m} mass loss rate), given as:

$$\frac{\int \dot{m} dA}{\int dA} \quad (2)$$

The addition of carbon vapors to the high temperature portion of the shock layer enhances the

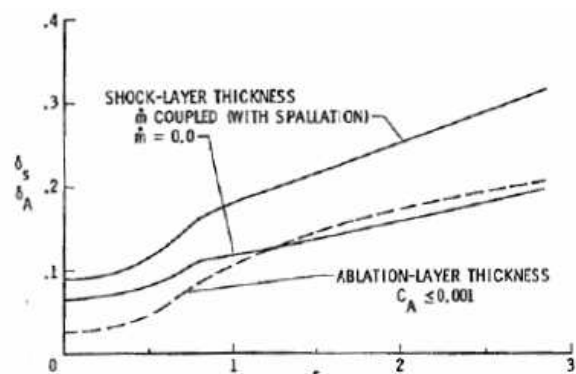


Figure 7: Shock layer and ablation layer thickness distribution (from Ref. 9)

radiative transport. Numerical simulations⁷⁻⁸ showed that turbulence has a pronounced adverse effect on the surface heating. The enhanced transport brings the high temperature shock layer closer to the surface, causing the dissociation of absorbing molecules.

The calculation with coupled spallation⁹ showed that the coupled heating for a given freestream condition is not influenced by additional blowing, possibly suggests that the increased blowing is ineffective in reducing the surface heating rate because the turbulence produces such a thin layer where significant absorption occurs.

In several studies⁷⁻⁹, the radiative heat-flux with coupled injection exceeded the corresponding values for no injection for much of the conical frustum. This effect, at least for large heating rate conditions, was shown to be clearly associated to the flow turbulence⁷ and to the thicker shock layer due to injection. The thickness of the shock layer predicted numerically with and without injection is displayed in Fig. 7.

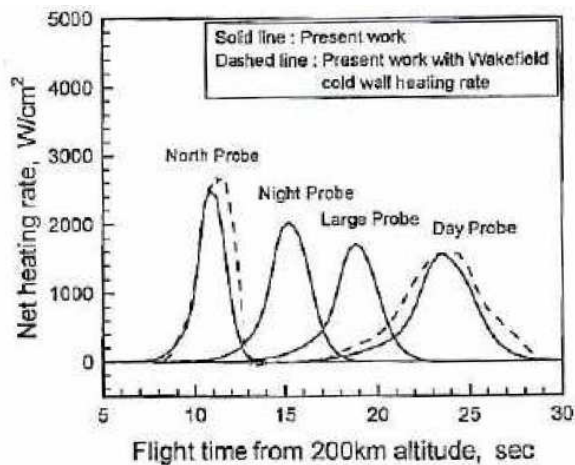


Figure 8: Net heating rates for the stagnation point of the Pioneer-Venus probes (from Ref. 19)

III. Pioneer-Venus

In 1978, four probe vehicles, called Pioneer-Venus probes (designated as Day, Night, Large and north probes), entered into Venus atmosphere at a speed of 11.5 km/s. The vehicles were protected by carbon-phenolic heat-shields equipped with thermocouples: one near the stagnation point and another at a point close to the frustum edge this for each probe. All thermocouples functioned during the mission, as well as the accelerometers for two of the four probes. A first attempt to rebuild the flight data¹⁶ with CMA¹⁷ was performed in 1980 but the calculated thermocouple temperature rose to unrealistic high values for both stagnation point and frustum edge¹⁸. Since then, in order to validate the tools and approaches, retained by JAXA for preparing the Hayabusa mission, several attempts have been performed to rebuild this data¹⁹⁻²⁰⁻²¹⁻²².

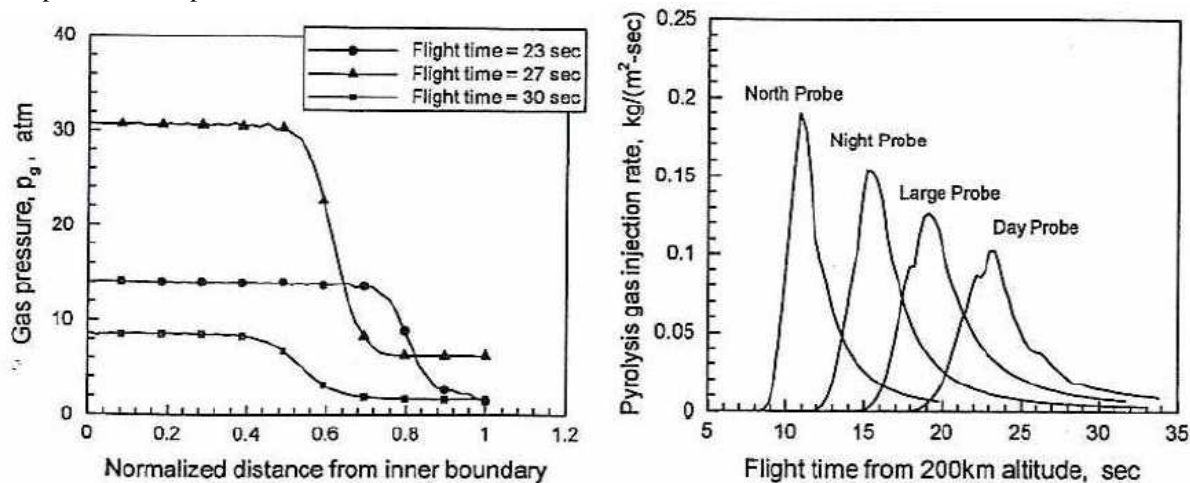


Figure 9: Left: Gas pressure inside the heat-shield for the day probe; Right: Pyrolysis gas injection rate (from Ref. 19)

In the perspective of the numerical rebuilding of ablative entries, one of the issues is the validity of a steady approach¹⁸. For Pioneer-Venus probes, due to the steep entry angles, the heating pulses for those vehicles were sudden (see Fig. 8) and, a priori, it is not evident that the assumption of steady-state pyrolysis was valid. When a virgin material is heated, the resin decomposes and vaporizes. As a result, gas bubbles are formed and become inevitably interconnected, so that the material becomes porous. In CMA, the pyrolysis gas escapes instantly. Under

this assumption, it does not affect the energy transport phenomenon. This assumption is valid if the thicknesses of the char and the pyrolysis zone are small. Such small thicknesses occur at very high pressure and high heating rate environment typical of missile warheads. At moderate pressure, this thickness is substantial. As a result, the pyrolysis gas spends a substantial time in travelling through these zones. During this travel, the pyrolysis gas absorbs energy and heat and thereby cools the material.

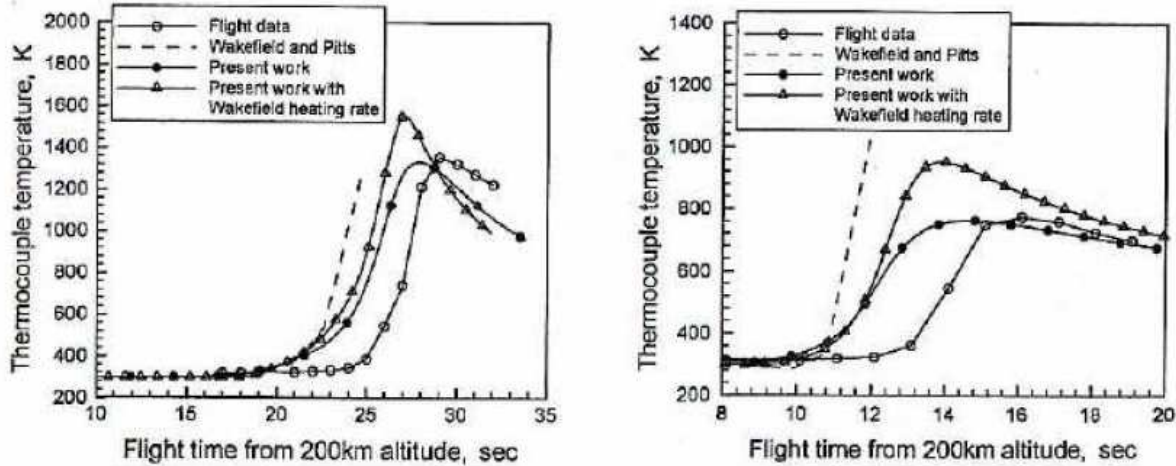


Figure 10: Comparisons between the calculated and measured temperature histories near the stagnation point for the Day (left) and North (right) probes (from Ref. 19)

As a consequence, an approach considering the char as a porous media¹⁹⁻²⁰ has been developed to rebuild the flight data. Equations based on Darcy law have been solved for the solid and gas phases. The governing equations are numerically stiff because of the source term accounting for pyrolysis. The approach was validated against the experimental data obtained in an arc-jet wind tunnel¹⁸ for the same type of carbon phenolic.

The gas pressure for the Day probe is reported in Fig. 9 with the pyrolysis gas injection rates for the four probes. The abrupt zone in the left part of this figure corresponds to the pyrolysis front. For Pioneer-Venus entry conditions, pyrolysis gas pressure reaches 30 atm¹⁹. Such a pressure may induce spallation. This agrees with other works²³ showing that the internal gas pressure in carbon-phenolic can be higher than 30 atm.

The thickness of the pyrolysis zone, after the peak heating when the thermocouple temperature is maximum for the Day probe, is in between 20% and 35% of the heat-shield depending on the predictions¹⁹⁻²⁰. The differences in the prediction of the pyrolysis zone thickness seem to originate from slight differences in the models used in these two studies.

The thermocouple temperatures have been rebuilt for the North and Day probes. The results obtained by Wakefield and Pitts¹⁸ and Ahn et al¹⁹ are reported in Fig. 10. The calculations performed by Wakefield and Pitts¹⁸ based on a steady state approach overpredict the temperature to exceed the melting point of the thermocouples. The method developed by Ahn et al¹⁹ led to a more realistic agreement, particularly for the slope and the peak values. For both probes, there is a tendency to predict the onset of temperature raise earlier in the trajectory than in the flight data. This might be due to the heat-transfer occurring at the thermocouple junctions or to clocking errors¹⁹.

The pyrolysis gas has a strong cooling effect on the surface temperature²⁰ with a maximum of difference of about 30% at the peak of the thermocouple temperature when this

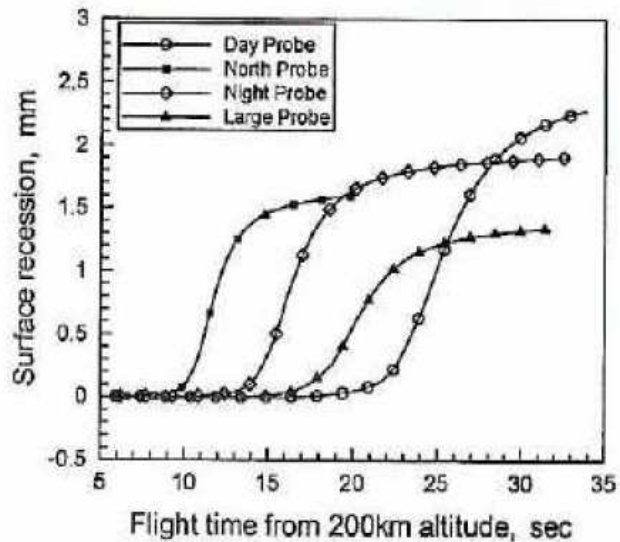


Figure 11: Calculated surface recession for the stagnation point of Pioneer-Venus probes¹⁹

phenomenon is considered. Accounting for the cooling effects of the pyrolysis gas²⁰ yields to a better agreement with the flight data obtained from the thermocouples than without¹⁸.

Some computations have been performed accounting for the convective blockage²⁰. This effect was included for the Large and Night probes and excluded for the Day and North probes. The choice done²⁰ was arbitrarily and reflects the uncertainty on a possible turbulent flow in the regions of measurement. Numerical simulations show a strong decrease of the heat-flux level when the blockage is taken into account with a drop in the range of 55-60% of the net heat flux²⁰, defined as the sum of the convective and radiative heat-fluxes minus the wall radiative cooling. Of course, in the case of a turbulent flow, this reduction is, at least, partially offset due to the increase in heat-transfer at the surface.

The calculated surface recession at the stagnation point due to the vaporization is presented in Fig. 11. From the four probes the Day probe is ablated the most severely by oxidation. Average recession for the heat-shield was around 2 mm.

IV. High-Speed Earth Re-Entry

A high speed Earth entry is much less ablative than a Jovian entry. However, for superorbital missions, such as sample return missions and manned missions to the Moon, ablation is a key issue. TPS recession was around 5mm with a charring of 2 cm for Apollo 4 (see Fig. 12). Some elements on blockage, related to high speed Earth entry, have been found in the literature and gathered hereafter. The review focuses on the flight and numerical data obtained in the context of high speed Earth entries performed for sample return and manned missions: Apollo, Genesis, Stardust, Muses and some Russian missions.

A. Apollo 4 and 6

To prepare the manned return capsule to the Moon, Apollo 4 and 6, two prototype vehicles, were flown in 1967 and 1968 respectively. They were instrumented with pressure sensors, several calorimeters (17 on the conical section and 10 on the aft section) and radiometers (4 radiometers) were embarked on-board²⁴. At least one calorimeter and radiometer were located close to the stagnation point.

Apollo TPS was made of AVCOAT²⁵ a highly ablative and catalytic material made of epoxy resin reinforced with quartz fibers and lightened with phenolic microballoons. The entry conditions were sufficiently severe to provoke a regime with a strong pyrolysis gas injection and char formation. The ground tests performed using AVCOAT²⁵ showed that for almost the test conditions, the material spalled.

For both vehicles, the radiometer produced reliable data (see Fig. 12) throughout the entry trajectory. However, the calorimeters provided reliable data only at the beginning of the flight because later on the signals exceeded the useful range of the sensors².

The entry velocity was 10.73 km/s for Apollo 4, with a peak heating at stagnation point around²⁶ 5 MW/m². For Apollo 6, the entry trajectory was degraded with an entry velocity of 9.5 km/s due to an unsuccessful attempt to reignite the Saturn 5 launcher.

Several studies have been dedicated to the numerical rebuilding of the flight data²⁴⁻²⁷. Numerical rebuilding of Apollo 4 and 6 entry aerothermodynamics were performed by Lee and Goodrich²⁴. Generally, the results compared fairly well with the flight data. The response of the ablative heat-shield during the entry was calculated by Curry and Stephens²⁶ and the predictions for surface recessions, char depths, and temperature histories at selected points are in good agreement with the flight data.

Due to the low entry velocity of Apollo 6, there are more studies in the literature focusing on Apollo 4. Recent studies have been performed using this data since this is the only flight data set for a high speed Earth entry available in the open literature. Numerical rebuilding of the stagnation-point heating rates

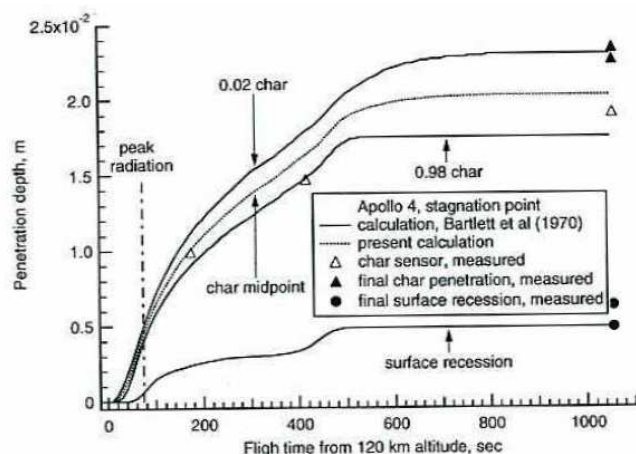


Figure 12: Rates of surface recession and charring at the stagnation point (from Ref. Erreur ! Signet non défini.)

of both Apollo 4 and 6 has been performed by Park and Tauber². A recent investigation on the stagnation point radiation for Apollo 4 has been conducted by Park²⁸, in this paper, details on heat-flux and analysis of surface recession and blowing rate history along the trajectory are also provided.

At the peak heating point of Apollo 4 entry trajectory, the convective and radiative heating rates were about 3.5 and 1.7 MW/m² at the stagnation point. However, about 2/3 of the convective heating rate was due to absorption of radiation in the boundary layer. The intrinsic components of convective and radiative heating rates were about 1.1 and 4.1 MW/m² respectively.

The injection rate of pyrolysis gas and the rate of vaporization of the heat-shield surface were obtained using char sensors and the distribution of the density of the heat-shield material in the recovered vehicle (Apollo 4). This leads to two sets of data for Apollo 4: one from the sensors during the flight and the second from the recovered heat-shield. These two sets of data were not consistent leading to two different values for both injection and vaporization rates. This data has been reviewed and discussed by Park^{Erreur ! Signet non défini.}, and then distributions of rates of surface vaporization and pyrolysis gas injection at the stagnation point have been derived from the data as shown in Fig. 13.

From the recovered heat-shield the rate of char material recession per meter of surface recession was 341.3 kg/m³. The rate of surface vaporization can be related to the rate of surface recession as follows,

$$\text{char vaporisation rate } m_s = \text{surface vaporisation} \times 341 \quad (3)$$

The rate of resin removal has been interpreted by Park^{Erreur ! Signet non défini.} to be the rate of injection of pyrolysis gas. The rate of resin removal per meter of char midpoint advance is 167.5 kg/m³. The rate of resin removal per meter of surface recession is 0.449×167.5 kg/m³. As a consequence, this author obtained:

$$\begin{aligned} \text{pyrolysis gas injection rate } m_p = & \text{char midpoint advance rate} \times 167 \\ & + \text{surface recession rate} \times 0.449 \times 167 \end{aligned} \quad (4)$$

The surface recession rate and the char midpoint advance rate were obtained by differentiating the surface recession value and the char midpoint value in Fig. 12. The resulting rates of char vaporization and pyrolysis gas injection are shown in Fig. 13.

B. Genesis

Little data is available in the literature on Genesis particularly for aerothermodynamics and heat-shield design; indeed most of the works performed on ablation and aerothermodynamics heating were not published²⁹. Some elements on ablation are available in this last paper.

Genesis heat-shield was made of carbon-carbon (fibers of highly ordered pyrolytic carbon) and was not equipped of sensors for the re-entry. The TPS had a thickness of 3.8 cm; the high density (1.8 g/cm³) material was highly conductive with a high surface temperature (2870 K).

The entry velocity of Genesis was slower than for Stardust and Hayabusa: 11 km/s against 12.9 km/s and 12.5 km/s respectively. Stardust arrives faster than Genesis and has a PICA³⁰ heat shield. Because of that, the peak surface temperature will not raise above 3500 K, temperature at which a convective surface layer of compounds (CO, C₃, air) carries away heat and in effect blocks boundary layer energy from reaching the surface.

The ablation rate has been studied from the signature of sodium traces in the heat shield material, calibrated by the total amount of matter lost from the recovered shield. According to Jenniskens et al.²⁹, most of the Genesis carbon-carbon heat shield is ablated over a period of about 40 seconds around peak heating. Most of the ablation would be due to oxidation, leading to CO and carbon atoms (from the decomposition of CO into C + O away from the surface). Peak ablation rate is 0.5 kg/s for Genesis (0.2 kg/s for Stardust) nearly of which goes into CO.

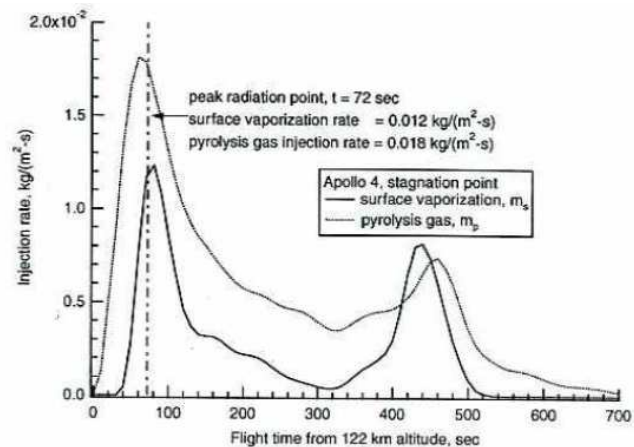


Figure 13: Rates of surface vaporization and pyrolysis gases at Apollo 4 stagnation point (from Ref. Erreur !

Radiation emission may be more intense for the Stardust re-entry, which is expected to ablate significant amounts of carbon in the form of atoms and C₃. Preliminary calculations of ablation products for Genesis show that CN Violet band around 400 nm may be detectable, even though abundances are expected to be low³¹. CN is generated from the interaction of carbon atoms from the surface with the nitrogen in the shock layer.

In the process of making the carbon-carbon, some binding component containing sodium left traces in the fibers. The measurements of sodium D-line intensity, even at a low rate, can be related to ablation. Sodium is an element that will rapidly ionize in the shock layer after leaving the surface. Hence, the intensity of sodium emission is expected to be proportional to the ablation rate.

C. Hayabusa (Muses-C)

The Hayabusa mission, also named Muses, is one of the most ambitious sample return mission ever performed. It is a sample return mission to the asteroid Nereus discovered in 1982. The return capsule is planned to perform a re-entry at 12.5 km/s in 2010 with a landing in Australia using a parachute. The allowable storing space for the capsule was very small: 40 cm in base diameter and 12 cm in depth with a allowed mass of 20 kg³². The small size or the return capsule was a strong constraint for the mission preparation.

For the trade-off of the TPS material, three candidates were selected:

- Carbon/carbon composite material backed by a low density silica insulator,
- Carbon phenolic as used for Galileo and Pioneer-Venus;
- A low-density carbon phenolic: PICA³⁰⁻³³.

At the time of the mission preparation, PICA was not flight qualified and not available in Japan. Carbon/carbon is known to better resist to high heating rates but tends to be heavy because of the back insulator. Finally, carbon phenolic was retained as baseline³² with a thickness of the heat-shield of 1cm, the mass of the heat-shield is 2kg.

Due to the lack of flight data for a high-speed Earth entry and to the similarity with a Venus entry, JAXA has undertaken a large effort based on the data obtained during the Pioneer-Venus mission, the tools used to design the TPS have been validated using the Pioneer-Venus flight data. TPS design numerical investigations have been performed accounting for surface combustion and convective blockage³². Convective heat-transfer has been calculated using a frozen boundary approach and radiative heat-transfer from published literature. The convective blockage was determined using the boundary layer equations through a similarity transformation. The approach was validated for carbon phenolic using Pioneer-Venus data. According to Ref. 32, in a CO₂ atmosphere with a carbon phenolic heat-shield the most significant reaction is the combustion of carbon producing CO. As a consequence, the rate of mass loss, \dot{m}_{ch} , of the char through combustion is,

$$\dot{m}_{ch} = \kappa \frac{\alpha_e^a}{1 + \frac{\kappa}{9.092 \beta \rho_w \sqrt{T_w}}} \quad (5)$$

Where T_w is the wall temperature, ρ_w the wall density, α_e^a is the species mass fraction of atomic oxygen at the boundary layer edge and β the reaction probability. κ is given as,

$$\kappa = 0.763 \chi Sc^{-0.6} (\rho_e \mu_e)^{1/2} \sqrt{\frac{du_e}{dx}} \quad (6)$$

Where χ is the convective blockage factor, Sc is the Schmidt number, μ_e the viscosity and u_e the velocity at the boundary layer edge.

The rate of heat-transfer through this process is,

$$q_{ch} = 2.2610^7 \kappa \frac{\alpha_e^a}{1 + \frac{\kappa}{9.092 \beta \rho_w \sqrt{T_w}}} \quad (7)$$

The wall value of atomic oxygen is computed by solving a diffusion equation as proposed by Goulard³⁴. The result is,

$$(\alpha_o)_w = \kappa \frac{\alpha_e^a}{1 + \frac{\kappa}{9.092 \beta \rho_w \sqrt{T_w}}} \quad (8)$$

Catalytic recombination of oxygen and nitrogen has been neglected, and surface nitridation was not observed. Carbon char sublimates and the main sublimation products is C_3 . The rate of mass loss by sublimation \dot{m}_s is expressed as,

$$\dot{m}_s = 6.061 \rho_w \sqrt{T_w} (\alpha_E^b - \alpha_w^b) \gamma \quad (9)$$

Where γ is the sublimation coefficient. For a smooth wall and C_3 its value is 0.03. For a rough wall, it has to be multiplied by the ration of the wet area to the projected area, with a final value about 0.1. By solving the Goulard diffusion equation and combining with the last one, the mass loss rate is,

$$\dot{m}_s = 2.2610^7 \kappa \frac{1.35910^{13} \gamma \sqrt{T_w} e^{-90845/T_w}}{\kappa + 6.061 \gamma \rho_w \sqrt{T_w}} \quad (10)$$

The heat transfer follows as,

$$q_s = H \dot{m}_s \quad (11)$$

Where $H = 1.693 \cdot 10^7$ J/kg.

Like for Pioneer-Venus, the flow was supposed to be laminar at the stagnation point but turbulent over the cone. For the design of the TPS, turbulent transition was assumed to occur instantly at the sonic line, at 30° location. Heat-fluxes were calculated at the stagnation and downstream points. The maximum was located at the downstream point due to the turbulent flow. The predictions of radiative flux reach a value of 4 MW/m^2 at the stagnation point while the total heat-flux is 12 MW/m^2 . At the frustum edge the maximum of heat-flux is 23 MW/m^2 due to turbulent heating.

The computations for response material predictions showed that the total ablated depth is 0.3 mm at the stagnation point and 0.58 mm at the downstream point. In the inner region the first 0.2 cm of the material turned into char while the pyrolysis does not occur deeper than 0.6 cm. At the frustum edge, the char thickness was nearly 0.5 cm and the pyrolysis stops at 0.2 cm from the inner boundary. According to these calculations, carbon phenolic was found to be a suitable material for MUSES-C.

D. Russian sample return missions

From the sixties to the eighties, Soviet Union had developed several exploration missions involving atmospheric entries. This was the case for Luna 16, a sample return mission to the Moon involving a high-speed Earth entry. The missions performed for Venus exploration such as Venera and Vega can also be cited. Unfortunately, there is no data available in the literature on the TPS materials used for the heat-shields, as well as on potential flight or experimental measurements.

However, in the last years, in the frame of the ISTC (International Science and Technology Centre) programme between Europe and Russia, some developments³⁵ have been done to assess the blockage for a Mars sample return mission.

Investigations on blockage have been performed for both Mars entry and high-speed Earth re-entry. The blowing effect on heterogeneous catalysis has been numerically and experimentally investigated for a Mars entry in Moscow at IPM³⁶. For a high-speed Earth entry, correlation for the convective blockage has been proposed and is detailed later on in this paper.

E. Stardust

The Stardust aerothermodynamics has been extensively investigated during the mission preparation and a large amount of numerical data is available in the literature. At 12.6 km/s, Stardust entry has been the fastest ever attempted into Earth atmosphere. The forebody TPS was made of PICA³⁰, a lightweight ceramic ablator close to carbon phenolic with the same elemental composition: 92% of carbon, 4.9% of oxygen, 2.2% of hydrogen and 0.9% of nitrogen. It is however less dense and has much lower thermal conductivity than carbon phenolic with the same ablation performance. Carbon phenolic has been developed to withstand very high pressures, of the order of 10 atm. For Stardust, the peak entry pressure was near 0.5 atm. Therefore, the high mechanical strength of carbon phenolic was not needed. In Stardust context, PICA was an enabling technology, because the mission cost and weight constraints could not have been met using a heavier carbon-phenolic heat-shield. The backcover was made of SLA 561³⁷, a silicone elastomeric material already used for the Viking probes and re-used for Mars-Pathfinder. The peak heat flux on the afterbody³¹ was almost two orders of magnitude less than the stagnation point heat flux.

The heat-flux during entry has been computed^{31,38} along the trajectory using a loosely coupled approach with radiation and ablation. The surface temperature and the coupled mass injection rate were calculated by iterating the solution of the flow-field and material response equations. Gupta³⁸ has only computed, while the afterbody with the

wake was also calculated by Olynick et al³¹. Flow-field calculations were based on 18 and 20 species chemical models in³¹ and³⁸ respectively. Computations were carried with and without accounting for ablation products. A significant difference between the two models is that the ions N_2^+ , O_2^+ and NO^+ were dropped from the 18-species model. Due to their small mass fraction in the flow, these ions were removed to decrease the computational cost.

According to Gupta³⁸, a non ablating surface using a fully catalytic wall condition (with complete recombination) may not be realistic at temperatures greater than 2000 K. A physically consistent boundary condition in this case would be an equilibrium catalytic wall, which would reduce to a fully catalytic boundary condition at lower temperatures (<2000 K). The other set of computations³⁸ were performed for a non catalytic wall, a fully catalytic wall and a wall at local equilibrium. Two boundary conditions were used by Gupta³¹: non ablative with a fully catalytic wall at radiative equilibrium for the forebody and the afterbody, and an ablative condition on the forebody with a fully catalytic wall at the forebody.

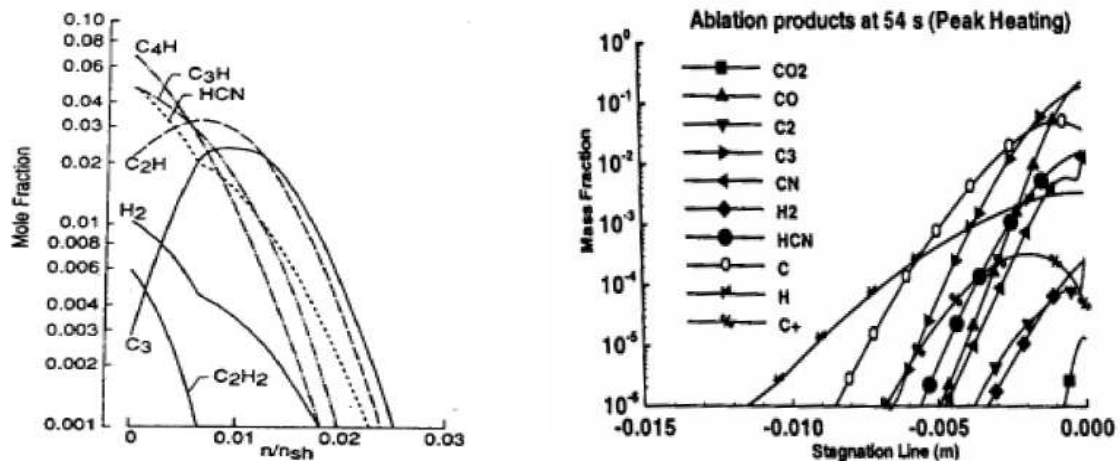


Figure 14: Left: Stagnation ablation species profiles at equilibrium (from Ref. 38) Right: Peak heating conditions computed (from Ref. 31)

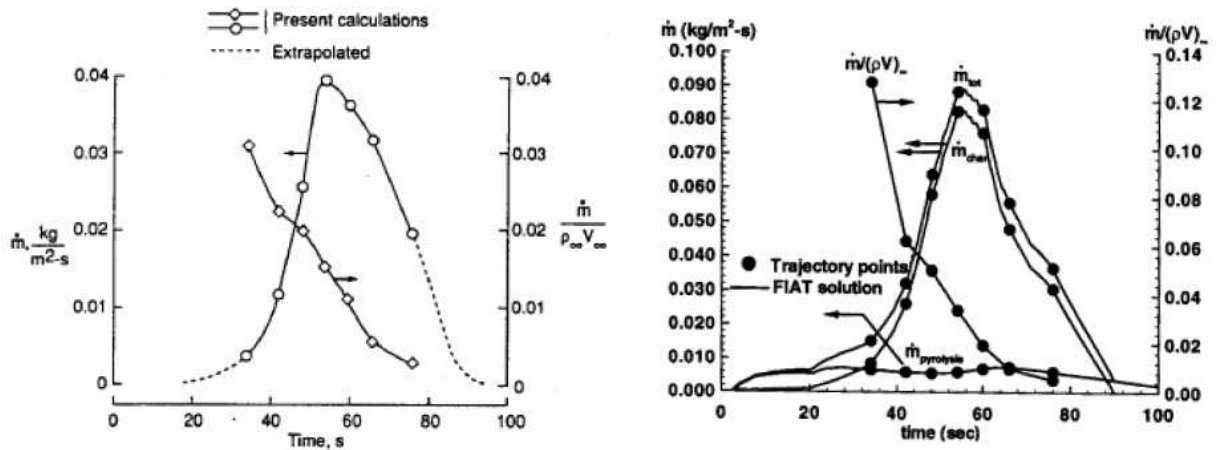


Figure 15: Stagnation blowing rate versus time predicted by Olynick et al³¹ (left) and Gupta³⁸ (right)

For most of the trajectory investigated^{31,38}, the surface temperatures are higher than 3000 K. Hence, the fully catalytic wall boundary condition is physically inappropriate since full recombination of air cannot be forced for temperature higher than 2000 K.

The ablation of SLA-561 was not considered by Olynick et al³¹ even if the afterbody heat-shield is ablating during entry. Fully catalytic simulations were performed to provide arc-jet test conditions while the ablative computations were used to size the heat-shield.

Gupta³⁸ to compute the radiative heat-flux has neglected the precursor effects and the freestream was considered to be cold and transparent. In the same study, C₃ was expected to be the main absorbing specie and its ultraviolet properties were taken from Shinn³⁹.

The ablation boundary conditions, namely blowing rate, species mass fractions and wall temperature, for the flow-field solution were obtained iteratively by assuming the surface composition to be in equilibrium at the temperatures and pressures predicted from a material response code (with inputs of wall heat transfer and pressure from the flow-field solution). The pyrolysis gas composition at the surface was obtained by assuming that the surface is in equilibrium at the local temperature and pressure.

According to Gupta³⁸, it was not obvious from the results of Park and Ahn²¹, how some of the pyrolysis species such as CH₂, CH₃, CH₄, and C₃ were accounted for. Molar fractions of ablation species are displayed in Fig. 14. The dominant ablation species from PICA are CO and C₃, secondary ablation products are C, HCN, CN and H. The blowing gases from PICA consist primarily of char with a small amount of pyrolysis gas.

The ablation injection, radiative transport and turbulence models are those retained by Gupta et al⁴⁰. For ablation injection a steady state is assumed. For the surface ablation cases considered in the present study, an energy balance at the flow-field ablator interface gives the coupled mass injection rate:

$$\dot{m} = \left(\frac{-q_w^R - q_w^C}{\sum_{i=1}^N (C_i h_i)_w - h_a} \right) \quad (12)$$

Where q_w^R is the radiative heat-flux at the wall, q_w^C the convective heat-flux, C_i and h_i the species mass fraction and species enthalpy respectively, and h_a , the enthalpy of undecomposed ablation material.

The stagnation blowing rates predicted along the trajectory^{31,38} are plotted in Fig. 15. At peak heating, where the peak mass injection rate occurs, the surface blowing rate is about 3% of the freestream mass flux³¹. In the same study, the maximum ratio, between the blowing rate and the freestream mass flux, occurs early in the trajectory and is about 13 %. Thus, the effects of the mass injection rate on the shock standoff distance are more pronounced earlier along the trajectory. There is a strong discrepancy between the computed values of the mass injection rates predicted in the two studies^{31,38}. The values obtained by Gupta³⁸ are half of those obtained by Olynick et al.³¹. These differences might be due to different surface elemental composition. The dominant ablation species, not included in³¹, are C₂H, C₃H and C₄H. Non inclusion of these species may be responsible for the differences with the mass loss rates obtained in³⁸.

Turbulent and laminar mass injection rates predicted by Gupta³⁸ are displayed in Fig. 16. The small injection rates are usually encountered before large scale oxidation and sublimation drive the species, due to the freestream, away from the surface. There was no noticeable effect of ablation injection and turbulence on surface pressure distribution.

The distributions of heat-flux along the surface at peak heating obtained by Gupta³⁸ and Olynick et al³¹ are displayed in Fig. 17. A maximum stagnation heating of about 11 MW/m² was obtained in [38] for the no ablation injection case with equilibrium flow chemistry and equilibrium catalytic wall boundary condition. The radiative equilibrium wall temperature was about 3800 K. A close value for the maximum peak heating, 12 MW/m², was obtained by Olynick et al.³¹. Results for a fully catalytic wall obtained in both studies^{31,38} are in good agreement. For both predictions with ablation injection, the predicted stagnation point heat-flux at peak heating is reduced by about 35 % (see Fig. 17). After peak heating, the blowing rate is lower as shown in Fig. 15, and the blockage by ablation is less effective. According to Olynick et al.³¹, reduction in heating due to ablation is slightly less downstream of the

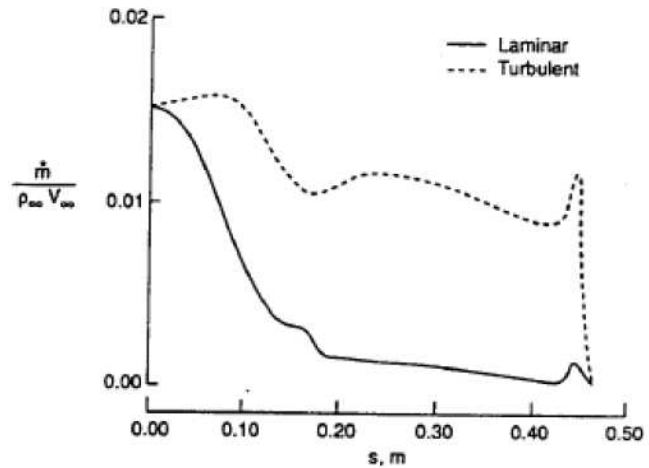


Figure 16: Mass injection rate distribution at peak heating³⁸

stagnation point, along the conical flank, and over the shoulder. For the ablation injection and turbulent flow solutions, the heating is reduced by only 13% on the conical flank and the shoulder comparing to a non-ablating laminar solution. On the left part of Fig. 17, the reduction in heating by ablation injection appears to be partially offset by the augmentation due to turbulence.

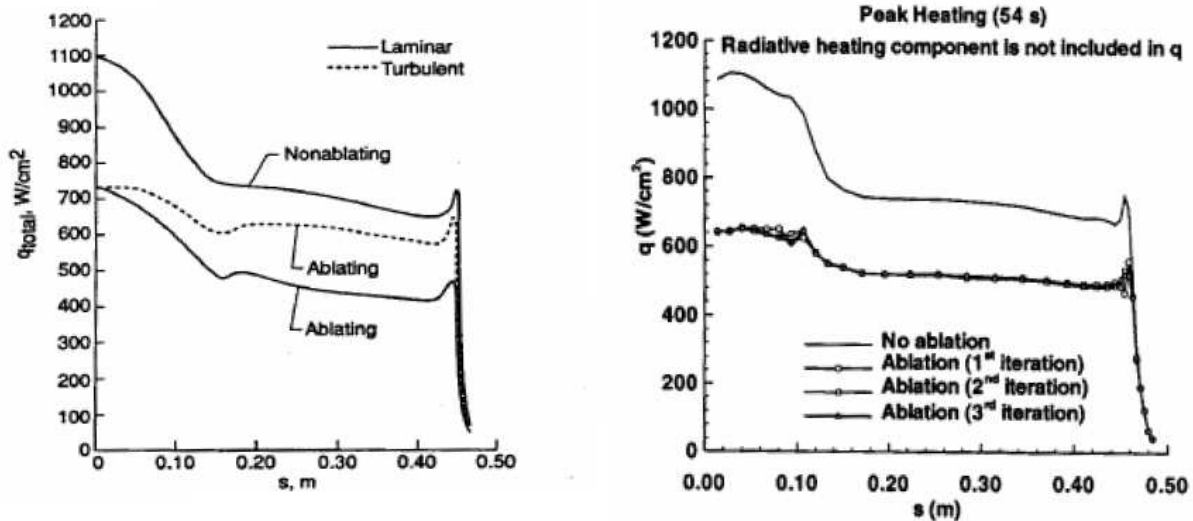


Figure 17: Total surface heat-flux distribution at peak heating conditions calculated by Gupta³⁸ (left) and Olynick et al³¹ (right)

The radiative heating for Stardust was around 10% of the total heating at the stagnation point and 7% at the shoulder³¹. Generally, the non-equilibrium effects should increase⁴¹ the radiative heating in comparison to the equilibrium value.

Ablation reduces the surface gradients of temperature and that of various species mass fractions, causing a decrease of convective and diffusive heat-fluxes. CO, one of the main ablation products, lowers significantly the wall enthalpy. There is a slight increase of radiation with ablation before the peak heating³⁸. A deeper penetration of the shock layer by the ablation species C and CO in the earlier time of the trajectory has been reported^{11,31}, and the increase in radiation from C lines and CO(4+) is only partially offset by the absorption of ablation species during that period.

Another effect of ablation is to reduce the surface shear by reducing the normal velocity gradient at the surface. In Fig. 18, the peak shear, located at the shoulder, is plotted versus time. The reduction of the peak shear due to ablation is equal to 25%. If the shear is too large and is beyond the material limits then spallation occurs. Surface recession predicted by Olynick et al.³¹ was about 1 cm at the stagnation point and 0.5 cm over the cone.

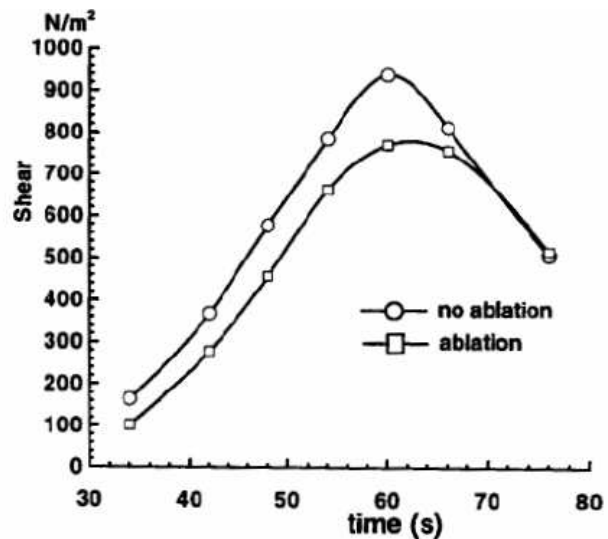


Figure 18: Comparison of non ablating and ablating peak surface shear versus time (from Ref. 31)

V. Modelling of the Convective Blockage

Most of the numerical data gathered during this review on convective blockage were related to two missions: Galileo and Stardust. For Galileo, the way to estimate the blockage or even the blowing rate was mostly based on semi-empirical correlations obtained from experimental and/or numerical results. For Stardust, 25 years later,

numerical predictions using coupled approach between CFD and material response codes were undertaken. In this section an assessment to predict the convective blockage is carried out based on the studies reported in the literature.

A. Convective blockage factor

The convective blockage factor, ψ_c , is a reduction function defined as,

$$C_w = \psi_c C_{w,o} \quad (13)$$

Where C_w is the convective heat transfer of the surface accounting for the blowing, while $C_{w,o}$ is the convective heat transfer for the non ablating surface.

From the relation (13) the heat-flux at the wall can be derived^{35,42} as,

$$q_c = C_w (h_o - h_w) \quad (14)$$

Where h_o is the total gas enthalpy and h_w is the enthalpy of the gas mixture in the boundary layer at the wall temperature.

The reduction function can be estimated using numerical simulations or from semi-empirical correlations. These two methods are described hereafter.

1. Semi-empirical correlations

Several correlations for ψ_c , established during the Galileo project, can be found in the literature (see section I). These correlations are semi-empirical and based on experimental or computational data valid only for Jupiter entry conditions and carbon-phenolic material. Some are valid for laminar flows, other for turbulent flows. They are function as the blowing rate factor determined using semi-empirical formula.

According to Duffa⁴³ a lot of empirical correlations that can be found in the literature, are of the type,

$$\psi_c = \frac{1}{1+\eta B'} \quad (15)$$

Where η is an arbitrarily parameter. B' , the non dimensional blowing rate is defined as,

$$B' = \frac{\dot{m}}{C_{w,o}} \quad (16)$$

Behind correlation (15) an important physical phenomenon is hidden: the separated flow for strong injections⁴³. For low Mach numbers and laminar flows, this effect can occur above $B' = 2.6$. This shows also that the Reynolds similarity is not valid for the strong injections: due to the separation, the friction coefficient is negative while the flux and the Stanton number are positive.

For the Muses-C project, Ahn and Park³² have derived a correlation (see §IV.C) based on the analysis of the main driven phenomena specific to carbon phenolic and Venus atmosphere. This correlation has a form similar to Equation (15). If the approach for establishing this correlation is attractive, the validity is restricted to the same TPS material performing a similar entry.

Another interesting correlation has been reported by Murzinov et al.⁴⁴ where the reduction factor is,

$$\psi_c = 1 - KB' \quad (17)$$

This correlation is valid for the moderate values of the non dimensional blowing rate B' ($B' \leq 1$). K is a constant close to 0.6 for a laminar flow⁴⁴.

A more generic blowing rate correction equation can be found^{43,45} and has also been used by Bianchi et al⁴⁶. The reduction factor ψ_c is given by,

$$\psi_c = \frac{\ln(1+2\lambda B')}{2\lambda B'} \quad (18)$$

Where λ is the blowing reduction parameter. For laminar flows its value is 0.5 and Equation (18) reduces to the classical laminar flow blowing equation⁴⁷. A variable is used for cases with transitional and turbulent flows. For laminar flows and the small values of B' , Equation (18) leads to,

$$\psi_c \approx 1 - 0.5B' \quad (19)$$

This equation for ψ_c is similar to the relation (17) with a value of K equal to 0.5 instead of 0.6. Using this approach, benchmark solutions were calculated and compared with available solutions for PICA⁴⁵. Code-to-code comparisons have shown consistency and accuracy for nosetip configuration made of different materials with PICA among them. A benchmark⁴⁶ has been performed between fully coupled ablative simulations and non ablative

predictions coupled to this approach. Numerical results have shown a very good agreement between the two approaches which demonstrates the interest of this method to account for convective blockage.

It does not seem to be generic specific correlations for turbulent flows. According to Duffa⁴³, based on comparisons between correlations and experimental results, the correlations used for laminar flows are still valid for the turbulent ones.

2. Numerical predictions

Another way to estimate the blowing factor is to perform numerical simulations. This way has been extensively used for Galileo⁵ to determine the convective blockage factor at the stagnation point. This task can be achieved through the fully coupling between a CFD and a material response code. Fully coupling or loosely coupling can be used; in both cases the hypothesis of a steady ablation state is generally assumed.

The loosely coupled approach is carried out as follows. The ablative species and the blowing rate are determined using a material response code. Then, a CFD code is needed where an ablative boundary is integrated. At this boundary, the blowing rate and the different species produced by the pyrolysis process are accounted for⁴⁸⁻⁴⁹.

In the case of the fully coupled approach, CFD and materials codes are interfaced. This method was used for Stardust^{31,38}. With the hypothesis of a steady ablation state, from the flow-field calculations, knowing the material composition and its sublimation temperature, the blowing rate and the gas species injected in the boundary layer can be predicted. Then, the flow-field is predicted accounting for the new boundary conditions at the wall and pyrolysis gas injection. The process is performed till the convergence of the solution which can be achieved in two passes^{31,38}. From the comparison between non-ablative predictions and coupled solutions the blockage factor can be assessed.

3. Stagnation point correlations

Among the studies performed in the frame of ISTC^{35,50}, several were focused on blockage for a Mars sample return mission. The effort has been put on stagnation point blockage and several correlations have been developed and validate using experimental tests performed in a plasmatron. One of the well known formulas⁵¹ for stagnation point blockage valid for a fully catalytic wall is,

$$\frac{q_w}{q_{w,o}} = 1 - 0.72 B + 0.13 B^2 \quad (20)$$

Where B is the blowing parameter defined as,

$$B = \frac{\rho_w U_w (h_e - h_w)}{q_{w,o}} \quad (21)$$

Where ρ_w , U_w and h_w are the wall density, velocity and enthalpy respectively, h_e is the enthalpy at the boundary layer edge.

According to Chernyi and Losev³⁵, this correlation is valid for different plasmatron power and injecting gases. However, this correlation is not valid for non catalytic walls. Using the same type approach and experimental tests, a correlation for a non-catalytic wall has been proposed^{35,50},

$$\frac{q_w}{q_{w,o}} = 1 - 1.1 B_f + 0.15 B_f^4 \quad (22)$$

With B_f defined as,

$$B_f = \frac{\rho_w U_w (h_e^f - h_w^f)}{q_{w,o}} \quad (23)$$

Here, h_e^f and h_w^f are the frozen enthalpy at the boundary layer edge.

The correlation (22) has also been validated for different plasmatron power and injected gases. However, at high power regimes with oxygen injection, this correlation is no more valid due to the intensive reduction of heat-flux (induced by the exchange reactions $O + N_2 \leftrightarrow NO + N$ and $NO + O \leftrightarrow N + O_2$).

B. Blowing rate

All the correlations for convective blockage gathered during this review depend on the blowing rate. There are many correlations for computing the blowing rate of an ablative material. Some of them are empirical and therefore

material dependent, other are based on surface energy balance at the material surface and are more generic. Semi-empirical correlations were extensively used for the Galileo project. For more recent studies the prediction of the blowing rate is mostly based on the energy balance at the wall.

In the perspective of the assessment of the blockage, the estimate of the blowing rate from material properties and flow conditions is the driving point. The blowing term represents the gaseous diffusion of the decomposing material into the boundary layer causing a thickening of the boundary layer and a reduction of the temperature gradient.

For Izawa and Sawada⁵², the blowing parameter B is the ratio of the injected mass rate to the fraction of the maximum available heat arriving at the surface without mass addition,

$$B = \frac{\dot{m} C_p (T_t - T_w)}{q_0} \quad (24)$$

Where T_t and T_w are the total and wall temperatures respectively, and C_p is the specific heat.

Two phenomena complicate the computation of blowing: the state of the pyrolysis gas, laminar or turbulent, and the spallation. For TPS sizing the prediction of the blowing rate is a critical point. Small changes in heating rate and surface temperature result in large changes in ablation and surface blowing rate⁴². The large changes in the blowing rate cause significant changes in subsequent heating rates that result in large oscillations in surface heating as the solution technique moves from trajectory point to trajectory point.

4. Galileo Background

Several modelling of the blowing rate have been proposed during Galileo project. In the case of Galileo, the prediction was more complex due to the problem of spallation. The first correlation found in the literature has been proposed by Moss & Simmonds⁹, according to them the mass injection rate is given by,

$$\dot{m} = \left(\frac{-q_w^R - q_w^C}{\sum_{i=1}^N (C_i h_i)_w - h_a} \right) + \dot{m}_{spl} \quad (25)$$

This expression is close to Equation (12) used during Stardust project, the only difference is the presence of an additional term representing spallation. The expressions for the ablation mass loss due to spallation were experimentally derived by Lundell⁵³. In these relations, the mass loss rate is proportional to the incident heat flux. The correlations for each of the heat-shield materials are given as,

$$\dot{m}_{spl} = 0.0099 (q_w - 145,0) \quad (26)$$

For the chopped-molded carbon phenolic of the nose cap, and as follows for the tape-wrapped carbon phenolic used at the frustum

$$\dot{m}_{spl} = 0.0073 (q_w - 85,0) \quad (27)$$

This modelling has not been retained for the post-flight analysis of Galileo entry performed by Matsuyama et al⁵⁴ where numerical simulations accounting for ablation and radiation have been carried out. For the boundary conditions, these authors have also assumed a steady ablation process. The injection rate was determined from an energy balance at the wall,

$$\dot{m} = \frac{-q_w^R - q_w^C}{\Delta H_a} \quad (28)$$

Where ΔH_a is the heat of ablation.

This approach is close to the correlation (25), however the effect of spallation is not accounted for. The wall temperature coincides with the sublimation temperature of the ablator. The sublimation temperature and the heat of ablation for the carbon phenolic⁹ (92% of carbon, 6% of oxygen and 2% of hydrogen in mass) are given by,

$$T_{sub} = 3797.0 + 342.0 \log p_w + 30.0 (\log p_w)^2 \quad (29)$$

$$\Delta H_a = 28.0 - 1.375 \log p_w + 27.2 (\log p_w)^2 \quad (30)$$

Where p_w is the wall pressure in atmospheres.

5. Other models

One of the first correlations found in the literature to model the blowing rate has been proposed by Metzger et al.⁵⁵. This correlation, based on experimental data, describes the ablation rate for graphite as,

$$\dot{m} (R/\rho)^{1/2} = 1.1910^6 e^{-22.14/T_w} \left\{ \frac{30.5}{R} + 4.8510^{15} \left(\frac{e^{-22.14/T_w}}{1 + 1.610^7 p^{-2/3} e^{-61.7/T_w}} \right)^2 \right\}^{-1/2} \quad (31)$$

Where R is the nose radius. This kind of correlation has a strong level of empiricism with a validity restricted to the same material for similar test conditions.

Another way is to determine the blowing rate from the surface recession rate Δs , defined by,

$$\Delta s = \frac{\dot{m}}{\rho_v} \quad (32)$$

Where ρ_v is the density of the virgin material. Here, a preliminary knowledge of the material for known entry conditions is required. It is a similar approach that was reported in § IV.A to analyze Apollo 4 re-entry from flight data.

Several correlations to predict the blowing have been established using boundary layer analysis. Such an approach⁵⁶ has been used to compute the blowing rate for an argon environment and carbon-based TPS. The boundary layer analysis leads to a global Knudsen-Langmuir equation for the ablation product species α ,

$$\dot{m} = \frac{\beta \rho_w C_w (\alpha_{E_w} - \alpha_w)}{4} \quad (33)$$

Where β is the vaporization coefficient, C_w the mean molecular speed of the ablation product species at wall temperature and the subscript E denotes equilibrium. The wall mass fraction is calculated from the equilibrium vapor pressure and the mean molecular weight. The equilibrium pressure is calculated as function of the wall temperature with an empirical correlation depending on the material.

This equation becomes for a helium atmosphere,

$$\dot{m} = \frac{\beta \rho_w M (p_E + p_w)}{4kT_w} \quad (34)$$

Where M and k are the mean molecular mass and the Boltzmann constant respectively, and p_E the wall pressure at equilibrium.

For the preparation of Muses-C re-entry Ahn & Park³² have developed an approach based on both theoretical analysis and empirical results. The prediction of the blowing rate is carried out through the analysis of the boundary layer assuming several hypotheses. Due to these hypotheses this approach is restricted to carbon-phenolic TPS and has been validated using Pioneer-Venus data. The hypotheses assumed are: low recombination of oxygen and nitrogen at the wall, interaction between carbon and oxygen only, non nitridation can be applied for an Earth high-speed entry; however the correlation developed is only valid for carbon phenolic and its application to another material might be questionable due to the hypothesis made.

C. Interaction with the char porous media

In material response codes, the charring phenomenon is usually calculated assuming that the pyrolysis gas escapes instantly. Under this assumption the pyrolysis gas, when formed, does not affect the transport phenomenon. Such assumption is valid if the thickness of the char layer is small. Such small thicknesses occur at very high pressures and high heating environment characteristics of military entries of nuclear warheads. For planetary entries, the pressures and heating rates are more moderate. As a consequence the char layer (and the pyrolysis zone) is less rapidly delaminated and can reach a substantial thickness. Then, the travelling time of the pyrolysis gas within the material is long enough for the gas to absorb heat and cools the material.

Hence, the behavior of the pyrolysis gas through the char layer has to be accounted for. Several numerical studies^{19,20,22} have been performed taking into account the porosity of the char material. All these investigations were focused on the rebuilding of Pioneer-Venus flight data. From the modelling point of view, new models and equations have to be solved to account for porosity. Models are needed for the void fraction inside the char material, tortuosity and permeability of the porous media, friction force. The mass flux, permeability and pressure of the pyrolysis gas have to be related by the Darcy law.

The material porosity has also an impact on the blowing rate modelling. According to Takahashi and Sawada²² the blowing rate can be modeled as,

$$\dot{m} = \varepsilon \rho_p U_p \quad (35)$$

Where ε is the char porosity, ρ_p the density of the pyrolysis gases and U_p the pyrolysis gas velocity. The density of the pyrolysis gases is,

$$\rho_p = \frac{P_w}{\sum_s \frac{C_{s,P}}{M_s} RT_w} \quad (36)$$

Where P_w and T_w are the wall pressure and temperature respectively, R is the gas constant, M_s is the molecular weight of species and $C_{s,p}$ the mass fraction of the species s in the pyrolysis gas.

D. Interaction with turbulence

It is known that transition to turbulence in supersonic flight occurs for a spherical body around the sonic point, located at an angle of 30° from the nose⁵⁷. During entries, transition to turbulence can occur at the stagnation point or in the downstream region over the cone surface. According to Ahn and Park³² this is due to: (1) the sphere-cone junction, that produces an unfavorable pressure gradient due to the disappearance of the centrifugal force there; (2) surface roughness due to ablation; and (3) possible spallation. As example, for Pioneer-Venus and MUSES-C the rate of ablation for low enough to maintain a laminar flow at stagnation point while over the cone surface the flow was most likely turbulent. The experiments with ablative blunt bodies have shown that turbulence can be high in the boundary layer when ablation occurs⁵⁸. The flow entering the boundary layer from the wall via ablation is already strongly turbulent and its turbulence intensity is driven more by ablation than by the boundary layer.

Most of the studies on the interaction between ablation and turbulence have been driven by the Galileo project. One of the main problems of Galileo post-flight analysis was to recover the correct material recession on the cone of the probe. This recession was higher than expected due to turbulence. The modelling of turbulence in the boundary layer in presence of injection of ablation products was pointed out⁵⁹ to be a clue for reproducing the flight data particularly at the frustum region. The main problem is that all the turbulence models have been developed for a smooth surface which is not the case for an ablative entry with a strong blowing of ablation products. In order to account for the blowing, Park⁵⁸ has proposed a correction of the classical modelling assuming that the turbulence intensity of the ablation products injected in the boundary layer was a function of the mass injection rate. Izawa and Sawada⁵² showed for a sphere with wall injection, that this model was able to reproduce the enhanced heat transfer rate at the stagnation point and that a higher heating rate in the downstream region was predicted. Using these different modelling for ablation and turbulence and accounting for radiation, Matsuyama et al⁵⁴ have performed several calculations of Galileo entry trajectory at thermochemical equilibrium. They were able to reproduce closely the flight data⁵⁹ for the surface recession as shown in Fig. 19. However, the recession in the frustum region is underestimated. The radiative heat-flux in this region can be increased if the presence of spalled particles is accounted for⁶⁰⁻⁶¹.

The convective blockage effect of ablation product gas becomes effective if the surface is covered by laminar injected gas. When turbulence comes out in the boundary layer, the amount of heat being transferred to the surface can be increased. It is well known, that the injection of foreign gas in the boundary layer through porous material promoted turbulence. Several experimental studies were conducted to evaluate the impact of injection on the boundary layer. Demetriades et al.⁶² demonstrated that the boundary-layer which is otherwise laminar, becomes turbulent when the injection rate increases. Kaattari⁶³ reaches the same conclusion, showing that the boundary layer is strongly turbulent at high injection rate. The results of Feldhuhn⁶⁴ showed that, if for the low mass injection rates the heat transfer is, in agreement with the laminar theory, reduced, while the high injection rates the heat transfer remains constant. Although the boundary layer theory can be extended to include the surface blowing²¹,

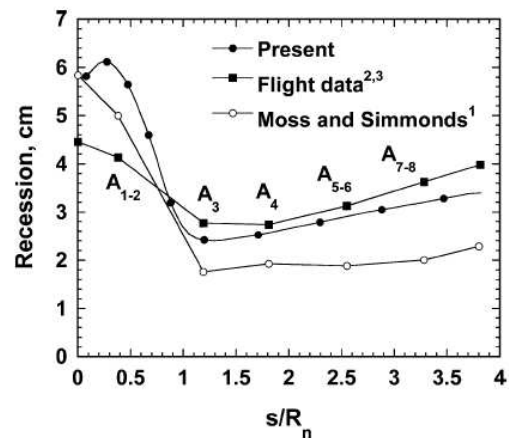


Figure 19: Comparison of obtained forebody recession profiles⁵⁴ with flight⁵⁹ and pre-flight data⁹ (from Ref. 54)

the prediction of heat-transfer rate for the ablative heat shield has inherent difficulties.

Turbulence may promote mixing of the ablation product gas with the air flow bringing the ablation products deeper into the interface region. Since the ablation products contain carbon, which tends to radiate strongly, the spallation phenomenon brings particles deep into the inviscid region that radiate.

VI. Conclusion

In this review, the experimental, numerical and in-flight data available in the literature related to the convective blockage has been gathered and a first analysis has been carried out. Most of the effort on blockage assessment found in the literature has been performed for the Galileo and Stardust projects. Some elements are also available for the other missions such as Pioneer-Venus, Apollo, Genesis and Hayabusa. Unfortunately, no available data was found for the missions developed by the former Soviet Union involving entries into Venus and Earth at superorbital velocity.

From the results obtained during the Stardust project and materials similar to PICA, the convective blockage can be estimated for a high-speed Earth entry, with a reduction of 35 % in convective heat-flux at the stagnation point and around 10 % at the leading edge. The decrease of the convective blockage along the cone is due to the presence of a turbulent flow since transition is most likely to occur during such an entry.

The correlations available for the blockage factor found in the literature have been collected. If most of them possess a high level of empiricism, others derived analytically from the energy balance at the wall are more generic and have been used for different studies performed in the frame of ISTC and Stardust. Such correlations depend on the blowing rate, which can be expressed as function of flow conditions and material properties (enthalpy of ablation, material species).

If this review seems to be one of the first efforts to gather the available data on convective blockage, some work has still to be performed. Some additional effort should be put to collect and review additional data and more effort has to be performed to analyse the correlations for blockage factor and blowing rate in order to establish a generic model for its assessment which would be useful for the preliminary design of heat-shield.

Acknowledgments

This work has been supported by the European Space Agency through ESA Consultancy Contracts 065/2006 and 067/2007. The author of this paper would like to thank Mr Heiko Ritter and Dr Lionel Marraffa from ESA/ESTEC as well as Dr Georges Duffa senior research scientist at CEA for their valuable advices and suggestions.

References

- ¹Laub, B., and Venkatapathy, E., "Thermal protection system technology and facility needs for demanding future planetary missions", *Proceedings of the International Workshop on Planetary Probe Atmospheric Entry and Descent Trajectory Analysis and Science*, ESA-SP544, Lisbon, 6-9 October, 2003.
- ²Park, C., and Tauber, M. E., "Heatshielding Problems of Planetary Entry, A Review", *30th AIAA Fluid Dynamics Conference*, AIAA Paper 99-3415, , Norfolk, VA, 28 June-1July, 1999.
- ³Holden, M. S., "Massive blowing from a heat shield during Jovian entry: An experimental study of the effects of large blowing rates on the character of the hypersonic shock layer", AIAA Paper 81-1070, June 1981.
- ⁴Moss, J. N., Jones, J. J., and Simmonds, A. L., "Radiative flux penetration through a blown shock layer for Jupiter entry", *2nd AIAA/ASME Thermophysics and Heat Transfer Conference* , AIAA Paper 78-908, Palo Alto, California, May 24-26, 1978.
- ⁵Brewer, R. A., and Brant, D. N., "Thermal protection system for the Galileo mission atmospheric entry probe", AIAA Paper 80-0358, Jan. 1980
- ⁶Brewer, R. A., Brant, D. N., and Fogaroli, R. P., "Development of a Steady-State Shape Change Ablation Code for the Design of Outer Planet Probes", AIAA Paper 77-95, January 1977.
- ⁷Moss, J. N., Simmonds, A. L., and Anderson, E. C., "Turbulent radiating shock layers with coupled ablation injection", *Journal of Spacecraft & Rockets*, Vol. 17, pp. 177-183, 1980.
- ⁸Moss, J. N., "A study of the aerothermal entry environment for the Galileo probe", AIAA Paper 79-1081, 1979.
- ⁹Moss, J. N., and Simmonds, A. L., "Galileo probe forebody flowfield predictions during Jupiter entry", *3rd Joint Thermophysics Fluids, Plasma and Heat Transfer Conference*, AIAA Paper 82-0874, St Louis, Missouri, June 7-11, 1982.
- ¹⁰Moss, J. N., Anderson, E. C., and Bolz, C. W., Viscous-Shock-Layer Solutions With Radiation and Ablation Injection for Jovian Entry, *AIAA 10th Thermophysics Conference*, AIAA Paper 75-671, Denver, CO, May 1975.
- ¹¹Moss, J. N., Anderson, E. C., and Bolz, C. W., "Aerothermal Environment for Jupiter Entry Probes", *11th Thermophysics Conference*, AIAA Paper 76-469, SanDiego, CA, June 1974.
- ¹²Jones, J. J., The Optical Absorption of Triatomic Carbon C₃ for the Wavelength Range 260 to 560 nm, NASA-TP-1141, 1978.
- ¹³Jones, J. J., "Shock Tube Measurements of the Optical Absorption of Triatomic Carbon, C₃", NASA TM-X-74025, 1974.

- ¹⁴Cooper, D. M., & Jones, J. J., "An experimental determination of the cross section of the Swings band system of C₃", *Journal of Quantitative Spectroscopy and Radiative Transfer*, Vol. 22(2), pp. 201-208, Aug. 1979.
- ¹⁵Brewer, L., & Engelke, J. L., "Spectrum of C₃", *Journal of Chemical Physics*, Vol. 36, February, 1962.
- ¹⁶Seiff, A., Kirk, D. B., Young, R. E., Blanchard, R. C., Findlay, J. T., Kelly, G. M., and Sommer, S. C., "Measurement of thermal structure and thermal contrasts in the atmosphere of Venus and related dynamical observations: Results from the four Pioneer-Venus probes", *Journal of Geophysical Research*, Vol. 85(A13), pp. 7903-7933, 1980.
- ¹⁷Kendall, R. M., Rindal, R. A., and Bartlett, E. P., "Thermochemical ablation", AIAA Paper 65-642, June 1965.
- ¹⁸Wakefield, R. M., and Pitts, W. C., "Analysis of the heat-shield experiment of Pioneer-Venus entry probes", AIAA Paper 80-1494, July 1980.
- ¹⁹Ahn, H.-K., Park, C., and Sawada, K., "Response of heatshield material at stagnation point of Pioneer-Venus probes", *Journal of Thermophysics and Heat Transfer*, Vol. 16(3), pp. 432-439, 2002.
- ²⁰Ahn, H.-K., Park, C., and Sawada, K., "Dynamics of pyrolysis gas in charring materials ablation", AIAA Paper 98-0165, 1998.
- ²¹Park, C., and Ahn, H. K., "Stagnation point heat transfer rates for Pioneer-Venus probes", AIAA Paper 98-0832, Jan. 1998.
- ²²Takahashi, M., and Sawada, K., "Simulation of entry flight flow-field over four probe vehicles in Pioneer-Venus mission", AIAA Paper 2002-0909, January 2002.
- ²³Shia, D., and McManus, H. L., "Modeling of composite ablators using massive parallel computers", AIAA Paper 95-1374, 1995.
- ²⁴Lee, D. B., and Goodrich, W. D., "The aerothermodynamic environment of the Apollo command module during superorbital entry", NASA TN-D-6792, April 1972.
- ²⁵Crouch, R. K., and Walberg, G. D., "An investigation on ablation behaviour of Avcoat 5026/39M over a wide range of thermal environments", NASA TM X-1778, Apr. 1969.
- ²⁶Curry, D. M., and Stephens, E. W., "Apollo ablator thermal performance at superorbital entry velocities", NASA TN D-5969, Sept. 1970.
- ²⁷Hillje, E. R., "Entry aerodynamics at lunar return conditions obtained from the flight of Apollo 4 (AS-501)", NASA TN D-5399, Oct. 1969.
- ²⁸Park, C., "Stagnation point radiation for Apollo 4", *Journal of Thermophysics and Heat Transfer*, Vol. 18(3), pp. 349-357, 2004.
- ²⁹Jenniskens, P., Wercinski, P., Olejniczak, J., Allen, G., Desai, P. N., Raiche, G., Kontinos, D., Revelle, D., Hatton, J., Baker, R. L., Russell, R. W., Taylor, M., and Rietmeijer, F., "Preparing for Hyperseed MAC: an observing campaign to monitor the entry of the Genesis sample return capsule", *Earth, Moon, and Planets*, Vol. 95, pp. 339-360, 2004.
- ³⁰Tran, H., Johnson, C., Rasky, D., Hui, F., Chen, H. K., and hus, M., "Phenolic impregnated carbon ablators (PICA) for Discovery class missions", AIAA Paper 96-1911, 1996.
- ³¹Olynick, D., Chen, Y.-K., and Tauber, M. E., "Aerothermodynamics of the Stardust sample return capsule", *Journal of Spacecraft and Rockets*, Vol. 36, pp. 422-462, 1999.
- ³²Ahn, H.-K., and Park, C., "Preliminary study of the MUSES-C reentry", AIAA Paper 97-0278, 1997.
- ³³Pallix, J., "High-temperature behaviour of advanced spacecraft TPS", NASA CR-195832, May 1994.
- ³⁴Goulard, R., "On catalytic recombination rates in hypersonic stagnation heat transfer", *Jet Propulsion*, pp. 737-74 Nov. 1958.
- ³⁵Chernyi, G. G., and Losev, S. A., "Problems of aerothermodynamics, radiation gasdynamics, heat and mass transfer for planet sample return missions", Final Project Technical Report of ISTC 1549-00, Research Institute of Mechanics, Moscow, Russia, June 2003.
- ³⁶Yakushin, M. I., Pershin, I. S., and Kolesnikov, A. F., "An experimental study of stagnation point heat transfer from high-enthalpy reacting gas flow to surface with catalysis and gas injection", In *Proceedings of the 4th European Symposium on Aerothermodynamics for Space Vehicles*, Capua, Italy, 15-18 Oct., 2001, ESA SP-487, March 2002.
- ³⁷Tran, H., Tauber, M., Henline, W., Tran, D., Cartledge, A., Hui, F., and Zimmerman, N., "Tests of SLA-561V heat shield material for Mars-Pathfinder", NASA TM 110402, Sept. 1996.
- ³⁸Gupta, R. N., "Aerothermodynamic analysis of Stardust sample return capsule with coupled radiation and ablation", AIAA Paper 99-0227, 1999.
- ³⁹Shinn, J. L., "Optical absorption of carbon and hydrogen species from shock heated acetylene and methane in the 135-220 m wavelength range", *Thermophysics of Atmospheric Entry*, edited by T. E. Horton, *Progress in Astronautics and Aeronautics*, Vol. 82, pp. 68-80, 1982.
- ⁴⁰Gupta, R. N., Lee, K. P., Moss, J. N., and Sutton, K., "Viscous shock-layer solutions with coupled radiation and ablation for Earth entry", *Journal of spacecraft and Rockets*, Vol. 29, pp. 173-181, 1992.
- ⁴¹Park, C., "Radiation enhancement by nonequilibrium in Earth's atmosphere", AIAA Paper 83-0410, Jan. 1988.
- ⁴²Kuntz, D. W., Hassan, B., and Potter, D. L., "Predictions of ablating hypersonic vehicles using an iterative coupled fluid/thermal approach", *Journal of Thermophysics and Heat Transfer*, Vol. 15(2), pp. 129-139, 2001.
- ⁴³Duffa, G., *Ablation*, Monographie, CEA-CEATA, Nov. 1996.
- ⁴⁴Murzinov, I. N., Rumynsky, A. N., Vlasov, V. I., Zalogin, G. N., and Knotko, V. B., "Earth entry of the vehicle with the Mars ground samples", *Proceedings of the 4th European Symposium on Aerothermodynamics for Space Vehicles*, Capua, Italy, 15-18 Oct., 2001, March 2002.

- ⁴⁵Chen, Y.-K., and Milos, F. S., “Two-dimensional implicit thermal response and ablation program for charring materials”, *Journal of Spacecraft and Rockets*, Vol. 38(4), pp. 473-481, 2001.
- [⁴⁶] Bianchi, D., Martelli, E., & Onofri, M., Practical Navier-Stokes computation of flowfields with ablation products injection, In Proceedings of 3rd TPS Workshop , ESTEC, May 2006.
- ⁴⁷Kays, W. M., and Crawford, M. E., “Convective Heat and Mass Transfer”, 2nd Edition, McGraw-Hill, New-York, 1980.
- ⁴⁸Smith, A. J., Bell, D., and Boulton, D., “TINA version 4, Theory and User Manual”, TN89/96 Issue 4, Fluid Gravity Engineering, Emsworth, United-Kingdown, Oct. 2002.
- ⁴⁹Reynier Ph., Marieu V., and Marraffa L., “Aerothermodynamics Developments for Planetary Missions”, In *Proceedings of the 1st Joint French-German Symposium on Simulation of Atmospheric Entries by Means of Ground Test Facilities*, SAE 99, pp. 2.5.1-2.5.8, Stuttgart, Nov. 17-19, 1999.
- ⁵⁰Yakushin, M. I., Pershin, I. S., and Kolesnikov, A. F., “An experimental study of stagnation point heat transfer from high-enthalpy reacting gas flow to surface with catalysis and gas injection”, *Proceedings of the 4th European Symposium on Aerothermodynamics for Space Vehicles, Capua, Italy*, 15-18 Oct., 2001, March 2002.
- ⁵¹Marvin, J. G., and Pope, R. B., “Laminar convective heating and ablation in the Mars atmosphere”, *AIAA Journal*, Vol. 5(2), pp. 240-248, 1967.
- ⁵²Izawa, Y., and Sawada, K.,” Calculation of surface heat transfer for a sphere with wall injection”, *Journal of Thermophysics and Heat Transfer*, Vol. 14(2), pp. 230-236, 2000.
- ⁵³Lundell, J., H., “Spallation of the Galileo probe heat shield”, AIAA Paper 82-0852, June 1982.
- ⁵⁴Matsuyama, S., Ohnishi, N., Sasoh, A., and Sawada, K., “Numerical simulations of Galileo probe entry flowfield with radiation and ablation”, *Journal of Thermophysics and Heat Transfer*, Vol. 19(1), pp. 28-35, 2005.
- ⁵⁵Metzer, J. W., Engel, M. J., and Diaconis, N. S., “Oxidation and sublimation of graphite in simulated re-entry environments”, *AIAA Journal*, Vol. 5, pp. 451-460, March 1967.
- ⁵⁶Park, C., “Stagnation-point ablation for carbonaceous flat disks – Part I: Theory”, *AIAA Journal*, Vol. 21(11), pp. 1588-1594, Nov. 1983.
- ⁵⁷Reda, D. C., “Correlation of nosetip boundary-layer transition data measured in ballistics-range experiments”, *AIAA Journal*, Vol. 19(3), pp. 329-339, March 1981.
- ⁵⁸Park, C., “Injection-Induced turbulence in stagnation point boundary layers”, *AIAA Journal*, Vol. 22(2), pp. 219-225, 1984.
- ⁵⁹Milos, F. S., “Galileo probe heat shield ablation experiments”, *Journal of Spacecraft and Rockets*, Vol. 34(6), pp.705-713, 1997.
- ⁶⁰Davies, C. B., and Park, C., “Trajectories of solid particles spalled from a carbonaceous heat shield”, *Progress in Astronautics*, Vol. 85, pp. 472-495, 1983.
- ⁶¹Park, C., “Radiation of spalled particles in shock layers”, *Journal of Thermophysics and Heat Transfer*, Vol. 18(4), pp. 519-526, 2004.
- ⁶²Demetriades, A., Laderman, A. J., Von Seggern, L., and Hopkins, A. T., “Effects of mass addition on the boundary layer of a hemisphere at Mach 6”, *Journal of Spacecraft and Rockets*, Vol. 13, pp. 508-509, Aug. 1976.
- ⁶³Kaattari, G. E., “Effects of simulated ablation gas injection on shock layer of blunt bodies at Mach 3 and 5”, NASA TN D-2954, 1965.
- ⁶⁴Feldhuhn, R. H., “Heat-transfer from a turbulent boundary layer on a porous sphere”, AIAA Paper 76-119, 1976.